J. Synchrotron Rad. (1995). **2**, 236–244

Use of Anomalous Diffraction, DAFS and DANES Techniques for Site-Selective Spectroscopy of Complex Oxides

J. Vacínová,[a] J. L. Hodeau,[a,b] P. Wolfers,[a] J. P. Lauriat[c] and E. ElKaïm[c]

[a]Laboratoire de Cristallographie CNRS, BP 166X, 38042 Grenoble CEDEX, France, [b]ESRF, BP 220, 38042 Grenoble CEDEX, France, and [c]LURE CNRS, Batiment 209D, 91405 Orsay CEDEX, France

(Received 27 February 1995; accepted 14 May 1995)

The diffraction anomalous fine structure (DAFS) technique is applied to highly absorbing 'real' crystals of arbitrary shape containing several heavy atoms. A multiwavelength refinement procedure of DAFS signals is demonstrated on two different oxides, $BaPt^{4+}_{1-2x}(Pt^{2+}_{1-y}Ba^{2+}_{y})_xO_{3-3x}$ with $x = 0.25$, $y \simeq 0$ and $BaZnFe_6O_{11}$, which have complex crystallographic structures. In these compounds, anomalous scatterers are located in different crystallographic sites and thus a multiwavelength refinement is necessary to separate out the site-selective information. An accurate absorption correction procedure for small, highly absorbing single crystals necessary for the DAFS analysis of this kind of samples is also presented.

Keywords: diffraction anomalous fine structure; anomalous scattering; absorption correction; multiwavelength refinement.

1. Introduction

Diffraction anomalous fine structure (DAFS) and diffraction anomalous near-edge structure (DANES) are both synchrotron radiation methods which simultaneously provide spectroscopic information regarding the local atomic environment of the 'edge atom' through X-ray absorption processes and long-range order information through diffraction processes. These techniques use the tuneable energy of the synchrotron radiation source to perform diffraction experiments near an absorption edge of a selected atom in the structure and thus make selective measurements possible.

The first DAFS oscillations were observed on diffracted intensities a long time ago (Cauchois & Bonnelle, 1956) but the experimental technique was only recently established by Stragier (1993) and Stagier, Cross, Rehr & Sorensen (1992) using a copper single crystal. They also demonstrated the valence sensitivity and site selectivity of the DAFS method using superconducting YBaCuO thin films. Even more recently, Pickering, Sansone, Marsch & George (1993) have shown the possibility of using the DAFS method with powdered samples to investigate local structural environments.

In contrast to previous works in which the materials studied by these methods have consisted mainly of multilayers, thin films, monoatomic compounds, powders or oxides in which individual site information is mainly extracted from pure, site-selective Bragg reflections, this work is focused on the study of highly absorbing single crystals with complex crystallographic structure. In these compounds, the edge atoms are located at different crystallographic sites. Each Bragg reflection receives contributions from several anomalous scatterers which are in inequivalent sites. To separate the individual site information, we have developed a simultaneous multiwavelength refinement procedure of several Bragg reflections with the anomalous terms f' of different crystallographic sites as unknowns. The anomalous terms f'', linked by f' through the Kramers–Kronig relationship, were calculated independently and introduced iteratively into the refinement. In the case of small, highly absorbing single crystals the principal variations of scattered intensity in the energy scan are produced by bulk absorption effects. For this reason, exact corrections for absorption are necessary before any analysis of anomalous scattering is made. In this paper we also present an absorption correction procedure which can be used for bulk absorption corrections of small, highly absorbing single crystals whose shape is irregular or poorly defined.

2. Experiment

2.1. *Samples*

For our synchrotron radiation experiments we have studied two single crystals of complex oxides: $BaPt^{4+}_{1-2x}(Pt^{2+}_{1-y}Ba^{2+}_{y})_xO_{3-3x}$ with $x = 0.25$, $y \simeq 0$ and $BaZnFe_6O_{11}$. In both cases, each compound has two different crystallographic sites occupied by anomalous scatterers (Pt atoms in the Ba–Pt–O compound, Fe in the Ba–Zn–Fe–O compound) and none of the Bragg reflections contain only contributions from the anomalous scatterers in a single specific site.

The structure of the first compound is twinned and can be described with the space group $C2$ with unit-cell parameters

$a = 17.460(4)$, $b = 10.085(2)$, $c = 8.614(3)$ Å (Vacínová, Hodeau & Chamberland, 1994). It is formed by a hexagonal compact packing of four BaO_3 layers *ABAB*, in which one of the four layers is deficient in oxygen. This packing along the *c* axis gives rise to a sequence of two face-sharing PtO_6 octahedra (O) occupied by Pt^{4+} cations connected with one trigonal prism (P), (–O–O–P– chains), occupied either with Pt^{2+} cations placed at the middle of one of three rectangular faces or Ba^{2+} cations placed in the centre of the prism. The single crystal chosen for synchrotron radiation experiments had the form of a small truncated hexagonal polyhedron of dimensions approximately 150 × 130 × 70 μm limited by its crystallographic faces.

The $BaZnFe_6O_{11}$ *Y*-type compound belongs to the hexagonal ferrite family. Its structure can be described with the space group $R\bar{3}m$ with cell parameters $a = 5.8723(1)$, $c = 43.556(2)$ Å. It is formed by a regular stacking of two different structural blocks (*S* and *T*) along the hexagonal *c* axis containing octahedral and tetrahedral sites (Collomb, Muller, Guitel & Desvignes, 1989). Each unit cell of this compound contains 30 Fe atoms distributed on four independent octahedral sites and six Fe atoms together with six Zn atoms on two independent tetrahedral sites (mixed occupancy). The large *c* cell parameter leads to a large number of accessible (00*l*) reflections. The single crystal used for synchrotron radiation experiments was a platelet (5 × 3 × 1 mm) with the (00*l*) scattering vector perpendicular to the largest surface.

2.2. *Data collection*

The anomalous diffraction and DAFS experiments were performed using classical monochromatic optics at wiggler line WDIF4C at LURE in Orsay, France. A double Si(111) crystal monochromator was used to produce an unfocused monochromatic beam. The samples were mounted on a four-circle diffractometer giving access to a large volume of reciprocal space. During the experiment at the Fe *K* edge with the Ba–Zn–Fe–O single crystal, the higher harmonics of the beam were almost completely removed by the combined effect of (i) a slight mis-setting of the second monochromator crystal, and (ii) the energy discrimination of the scintillation-counter signals. The diffracted intensities *versus* energy of several Bragg reflections were collected with a 2 eV energy step in the XANES (X-ray absorption near-edge structure) region and 4 eV step in the EXAFS (extended X-ray absorption fine structure) region. At each energy point all selected Bragg reflections were measured successively (because the experimental station WDIF4C was initially designed for monochromatic experiments). The energy range measured for the Ba–Pt–O single crystal was 11500–11700 eV around the Pt L_{III} absorption edge, and for the Ba–Zn–Fe–O crystal was 6900–7700 eV around the Fe *K* edge. The monochromator energy was calibrated by measuring the absorption edges of a platinum foil (11564 eV) and an iron foil (7112 eV) (Bearden & Burr, 1967). The calibration was stable during each experimental run (energy shifts less than 1 eV) and after each new reinjection a maximum energy shift of 2 eV was observed. During both anomalous diffraction experiments the absorption was measured in fluorescence mode simultaneously with the Bragg intensity measurements. The complementary fluorescence measurement is very important for energy calibration during the data collection. In addition, in the case of a small highly absorbing single crystal completely bathed in the beam, the fluorescence data can be used as a monitor of the incident beam intensity really received by the sample. An example of a raw DAFS spectra together with the fluorescence signal *versus* energy is shown in Fig. 1.

For both samples Bragg intensities were collected by a complete ω scan. This procedure is necessary when, due to the sample mosaicity, the peak shape is ill-defined and cannot be represented by a regular geometrical shape. This could be the case for compounds having structures containing finite size domains or twins. At the absorption edge the contribution of different domains to the diffracted

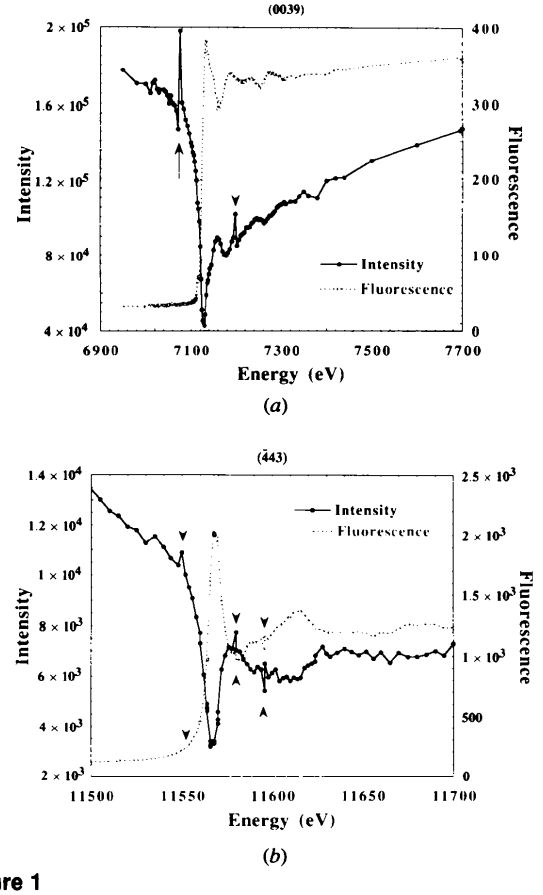

Figure 1
(*a*) DAFS spectrum of the (0039) Bragg reflection together with fluorescence signal *versus* energy measured in monochromatic mode on the large single crystal of Ba–Zn–Fe–O. Owing to the large unit-cell parameter *c* we observed 'glitches' at some energy points corresponding to multiple diffraction within the sample itself. (*b*) DAFS spectrum of the (4̄43) Bragg reflection together with fluorescence signal *versus* energy measured in monochromatic mode on the small single crystal of Ba–Pt–O. During the data collection we observed strong correlated variation of the diffracted intensity and the fluorescence due to beam inhomogenities (arrows).

intensity can vary because of reabsorption. For the Ba–Pt–O single crystal we have observed a variation of the peak shape with the energy which is caused by the variation of the contributions from twinned domains having different orientations with respect to the beam path (Fig. 2). A full profile integration procedure was also necessary because the Ba–Pt–O compound contains a basic structure and a superstructure having Bragg peaks with different half-widths. In this case, the peak height intensity is not proportional to the integrated intensity (Fig. 3).

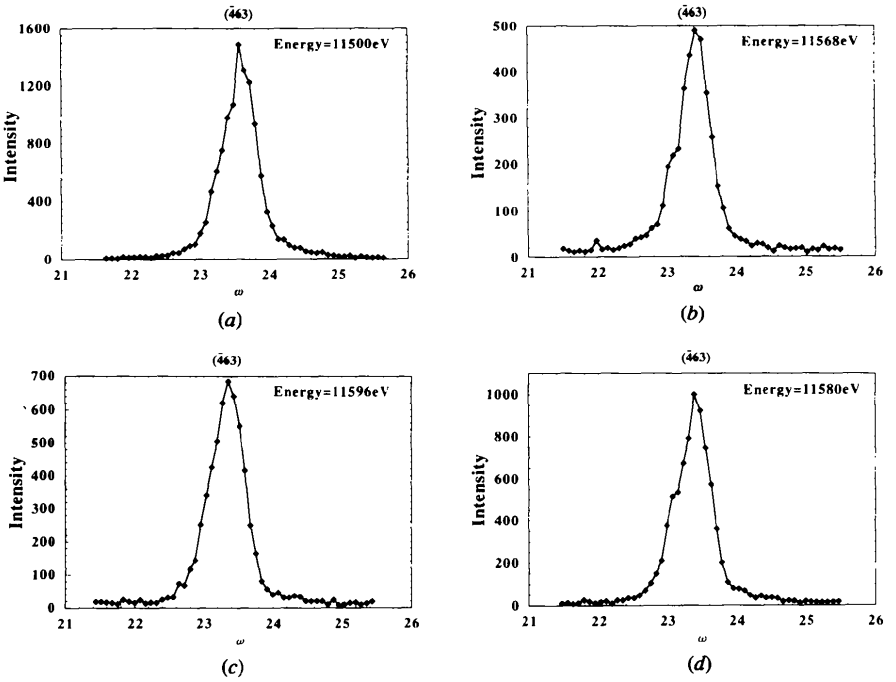

Figure 2
(*a*)–(*d*) Peak-shape variation of the (4̄63) Bragg reflection with the energy of the Ba–Pt–O compound caused by the variation of the contributions from twinned domains.

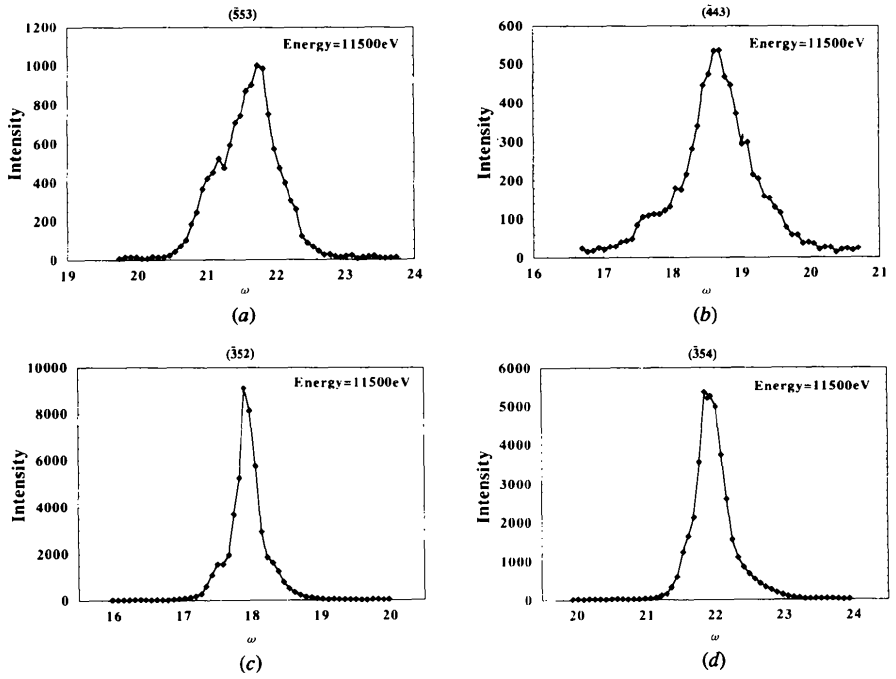

Figure 3
Peak-shape profiles of different Bragg reflections of the Ba–Pt–O compound at the same energy point (11500 eV) before the absorption edge: (*a*), (*b*) superstructure reflections; (*c*), (*d*) basic structure reflections.

This effect of the peak shape variation was not present in the Ba–Zn–Fe–O crystal, however, we have recorded complete ω scans anyway since they produce better data than is obtained by measurements of only the peak height intensity.

3. Data analysis

The atomic scattering factor of an atom A in the vicinity of an allowed electronic transition of the atom A can be written in the following form:

$$f_A(E) = f_A^0 + f_A'(E) + if_A''(E) \tag{1}$$

where f_A^0 is the normal scattering factor, f_A' and f_A'' are the real and imaginary anomalous dispersion corrections of the atomic scattering factor, and E is the energy of the incident beam. The anomalous imaginary term f_A'' is directly proportional to the atomic cross section σ_A:

$$f_A''(E) = (mcE/2he^2)\sigma_A(E) \tag{2}$$

where m is the electron mass, c is the velocity of light, e is the electron charge and h is the Planck constant. The term f' is related to f'' *via* the Kramers–Kronig relationship

$$f_A'(E) = (2/\pi)\int_0^\infty [E' f_A''(E')/(E^2 - E'^2)]\mathrm{d}E'. \tag{3}$$

In the vicinity of an absorption edge of one atom A in the compound, the total structure factor can be separated into two parts. The first part exhibits only the normal, smooth variation with energy of the anomalous terms f', f'' of the non-edge atoms. The second part contains a strong energy variation due to variations with energy of anomalous scattering factors f_A' and f_A'' of edge atoms. If all anomalous atoms A are identical, the structure factor can be written at a given energy E and for a particular reciprocal lattice node **h** as

$$F(\mathbf{h}, E) = F_T \exp(i\Phi_T) + \frac{[f_A'(E) + if_A''(E)]}{f_A^0} F_A \exp(i\Phi_A) \tag{4}$$

where $F_T \exp(i\Phi_T)$ is the normal contribution of *all* atoms in the unit cell to the structure factor and $F_A \exp(i\Phi_A)$ is the normal contribution of anomalous atoms A. Then the intensity of the Bragg reflection **h** for the compound containing identical anomalous scatterers A is proportional to:

$$I(\mathbf{h}) = C(ABS)LPD\lambda^3 \left[|F_T|^2 + \frac{(f_A'^2 + f_A''^2)}{(f_A^0)^2} |F_A|^2 + 2\frac{f_A'}{f_A^0}|F_T||F_A|\cos(\Delta\Phi) + 2\frac{f_A''}{f_A^0}|F_T||F_A|\sin(\Delta\Phi) \right] \tag{5}$$

where C is a scale factor, ABS is the bulk absorbance of the sample together with the geometrical effects, L is the Lorentz factor, P is a correction for the beam polarization, D is a correction for the detector efficiency and air absorption and $\Delta\Phi = \Phi_T - \Phi_A$ corresponds to the phase difference between the normal and anomalous parts of the structure factor. It is clear from (5) that it is more convenient to observe the energy variation of anomalous terms f_A' and f_A'' at Bragg reflections having a weak contribution of $|F_T|$.

The measurement of diffracted intensities of M Bragg reflections at k different energy points provides kM observations. If we then take a complex structure containing j different crystallographic sites for an anomalous scatter A (this means we suppose j different anomalous scatterers A_j of the same chemical nature but in different local environments or valence states), we will have for each energy point $2j$ unknowns $f_{Aj}'(E_k)$, $f_{Aj}''(E_k)$ which are not independent since they are related by the Kramers–Kronig relation. Supposing $kM > 2jk$ then the problem reduces to finding solutions for a non-linear set of kM equations based on (5) generalized for different anomalous scatterers A_j with $2jk$ unknowns.

In the majority of cases, the sensitivity of a Bragg reflection to the f'' term is much weaker than to the f' term and hence the independent refinement of the f'' terms becomes impossible. This problem can be avoided by reducing the number of unknowns in the system of equations to jk by using an iterative method for the refinement of $f_{Aj}'(E_k)$ and the calculation of $f_{Aj}''(E_k)$ by the Kramers–Kronig relation after each cycle of refinement.

After reducing the data collected at different energies to a common scale factor (which is refined together with the detector efficiency and the air absorption factor D in the energy region which excludes the highly structured region near the absorption edge) the calculations proceed in the following way:

(1) Bulk absorbance (ABS) and Lorentz–polarization (LP) corrections to the diffracted intensities in the entire energy interval are made.

(2) The individual complex correction factor for each Bragg reflection **h** is introduced.

(3) The anomalous scattering factors $f_{Aj}'(E_k)$ for the atoms A in the different crystallographic sites j are refined simultaneously and the factors $f_{Aj}''(E_k)$ are calculated by the Kramers–Kronig relationship.

3.1. *Angular and absorption correction of diffracted intensity*

The measured intensity of the Bragg reflections is affected by the Lorentz factor and the polarization factor. During our synchrotron measurements we have worked in the orbit plane where the incident radiation is $\sim 95\%$ linearly polarized.

The scattered intensities must also be corrected for bulk absorption effects. In the case of the Ba–Z–Fe–O single crystal, the Bragg intensities were measured in Bragg bisecting geometry with the scattering vector perpendicular to the flat face. The term ABS containing the absorption and geometrical effects is, for this sample, given by $ABS = 1/2\mu$. The linear absorption coefficient μ was

calculated using:

$$\mu(E) = [42081.1\rho/E(\text{keV})]\left(\sum c_i f_i'' / \sum c_i a_i\right) \quad (6)$$

where ρ is the density of the sample, a_i is the atomic weight of element i and c_i is the concentration of the ith element in the compound. The anomalous terms f_i'' for the non-edge elements were taken from Sasaki's tables calculated for free atoms using the Cromer–Libermann method (Sasaki, 1984). The term f_{Fe}'' was obtained from the absorption transmission experiment performed with a powdered sample. In the case of the Ba–Pt–O sample we cannot express the absorbance *ABS* in a simple form because of the small size of the crystal and its irregular shape. Instead, we have derived an empirical bulk absorption correction as described below.

3.1.1. *Empirical absorption correction procedure for a small highly absorbing single crystal.* As already mentioned, the single crystal of Ba–Pt–O has the form of a small truncated hexagonal polyhedron limited by its crystallographic faces. Because of the limited validity of the approximation $\mu \simeq I_f/I_0$ (where I_0 is the incident beam intensity and I_f is the intensity of fluorescence signal) in the case of small, highly absorbing samples (Pease, Brewe, Tan & Budnik, 1989; Tröger *et al.*, 1992), we could not obtain f_{Pt}'' directly from the fluorescence measurement. The average term f_{Pt}'' used for the absorption corrections was extracted from the XAFS spectra measured in transmission mode with a powdered sample. The first bulk absorption corrections were calculated by a program using the morphological description of the crystal by its faces. We have performed two different calculations for the absorbance *ABS*. First, with the same crystal description as for the structural refinement (Vacínová, Hodeau & Chamberland, 1994), and secondly with the distances of all crystallographic faces from the centre of the crystal 1 μm shorter (1 μm corresponds approximately to the error in determination of the crystal size). These calculations give significant variations of the absorbance (between 7 and 15%) which are greater than the DAFS signal and, for this reason, this method of absorption correction is not suitable for the DAFS data treatment.

The aim of the following procedure is to describe the absorbance *ABS* as a function of the linear absorption coefficient $\mu(E)$, the concentration of barium in prismatic sites (y), the X-ray beam path in the crystal (t) and its variation (Δt) with respect to the calculated path. The variable coefficients in the absorbance function must not affect the DAFS information and they are refined in the energy range far from the absorption edge where no oscillation occurs. Using the general non-stoichiometric formula $BaPt^{4+}_{1-2x}(Pt^{2+}_{1-y}Ba^{2+}_{y})_xO_{3-3x}$ in equation (6) we have calculated the linear coefficient μ for different values of y and we can describe the coefficient $\mu(y, E)$ as a linear function of $\mu(y = 0, E)$ and the concentration of Ba in prismatic sites y with a relative precision equal to 0.4% in the simple form

$$\mu(y, E_k) = c_1 y + (1 - c_2 y)\mu(0, E_k) \quad (7)$$

where c_1 and c_2 are constant, and E_k is the energy. If we express the absorbance *ABS* in the simple form

$$ABS(y, E_k, t) = \exp[-\mu(y, E_k)t(\mathbf{h}, y, E_k)], \quad (8)$$

then using the crystal shape, we can calculate the beam paths in the crystal for the different Bragg reflections **h** as a function of the linear absorption coefficient μ (Fig. 4).

From the calculated variation of the beam paths for the different Bragg reflections and different crystal shapes, we can assume that the path of one reflection **h** can be expressed as a sum of a 'model path t_m' common for all reflections and an energy independent constant term $\Delta t(\mathbf{h})$ corresponding to the difference between the lengths of the model path and the real path of the beam in the crystal for the reflection **h**. So we have expressed the beam path of the reflection **h** as

$$\begin{aligned} t(\mathbf{h}, y, E_k) &= t_m[\mu(0, E_k), y] + \Delta t(\mathbf{h}) \\ &= k_0(y) + k_1(y)\mu(0, E_k) \\ &\quad + k_2(y)\mu^2(0, E_k) + \Delta t(\mathbf{h}) \end{aligned} \quad (9)$$

where a 'model path' t_m is written using the polynomial function $\sum k_i \mu^i(0, E_k)$. The coefficients k_i are y-dependent and describe the variation of the 'model path' with occupation of Ba in prismatic sites y. Using the atomic positions of the refined structure (Vacínová, Hodeau & Chamberland, 1994) we refined the terms $\Delta t(\mathbf{h})$ and y simultaneously for all 22 measured Bragg reflections in the energy interval $E < E_0$; $E > E_0 + 60$ eV, where E_0 is the energy of absorption threshold, which excludes the highly structured region near the absorption edge. The refinements were performed with the program *MXD* (Wolfers, 1990) with a weighted least-squares agreement factor $R = 4.7\%$. The occupation of Ba in prismatic sites was $y = 0.08(2)$ [the value of y obtained from a monochromatic structural refinement with 5548 independent reflections was 0.043 (6) (Vacínová, Hodeau & Chamberland, 1994)] and $\Delta t(\mathbf{h})$ varied between reflections by ±7 μm. Although more peaks

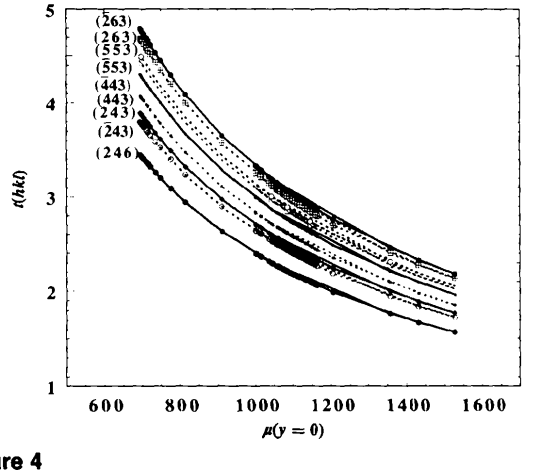

Figure 4
Beam paths of the Bragg reflections (*hkl*) as a function of linear absorption coefficient μ calculated from the morphological description of the crystal.

were measured in the original structural refinement, the high sensitivity of the anomalous scattering techniques to mixed site occupancy makes the new value $y = 0.08(2)$ more reliable. Two examples of the final fits of intensity applying the Lorentz–polarization, absorption and detector efficiency corrections are shown in Fig. 5.

3.2. *Multiwavelength refinement of Bragg reflection intensities and introduction of complex correction factor*

When we use the atomic positions and thermal factors determined by the monochromatic refinement, the calculated structure factor is accurate within a few percent for each reflection. Such accuracy is insufficient for the analysis of anomalous scattering data since it is the same order of magnitude as the DAFS oscillations. For strong reflections, this discrepancy, which could correspond to an inaccuracy in the determination of crystallographic parameters, is almost constant with energy. If we do not correct this inaccuracy we introduce systematic errors in f' and f'' calculations not only at the edge position but also in the region far from the edge. One way to avoid the systematic errors in f', f'' determination is to introduce a complex correction factor for the non-anomalous part F_N (F_N corresponds to the contribution of non-anomalous atoms to the structure factor) and refine this complex correction factor at energy intervals far from the absorption edge.

The introduction of the complex correction factor $\Delta F_N(\mathbf{h})\exp[i\Delta\varphi_N(\mathbf{h})]$, which is independent of energy, for each individual Bragg reflection is represented by $2M$ unknowns $\Delta F_N(\mathbf{h})$ and $\Delta\varphi_N(\mathbf{h})$ (M is the number of measured Bragg reflections). The structure factor for the Bragg reflection $\mathbf{h}$ corrected by this complex correction factor has the following form:

$$F(\mathbf{h}) = |F_N|\exp(i\Phi_N)|\Delta F_N|\exp(i\Delta\varphi_N) + \sum_j (f_A^0 + f'_{Aj} + if''_{Aj})\exp(2\pi i\mathbf{h}\mathbf{r}_j)\exp(-B_j h^2) \quad (10)$$

where $|F_N|\exp(i\Phi_N)$ is the contribution of all the non-anomalously scattering atoms to the structure factor. The system of $2M$ unknowns is solved for the same energy range as was used for the absorption corrections ($E < E_0$; $E > E_0 + 60\,\text{eV}$) where the anomalous $f'_{Aj}(E_k)$ and $f''_{Aj}(E_k)$ factors are included as known coefficients. In this energy range they are presumed to be equal for all crystallographic sites and their average $f''_A(E)$ values were taken either from theoretical curves for the free atom (Sasaki, 1984) or from the absorption transmission experiment with the powdered sample and average $f'_A(E)$ values were calculated by the Kramers–Kronig relationship.

All the Kramers–Kronig mutual transformations were performed by the method of integration developed by Templeton & Templeton (1988) with the differences $\delta f = f_{\text{exp}} - f_{\text{theor}}$ which tend to zero away from the experimentally measured absorption edge. The term f''_{theor} was obtained by modulating the anomalous factor f'' for the free atom (Sasaki, 1984) in the position of the absorption threshold with the arctan function as described by De Bergevin *et al.* (1992). The relativistic corrections proposed by Kissel & Pratt (1990) were also taken into account during the calculations.

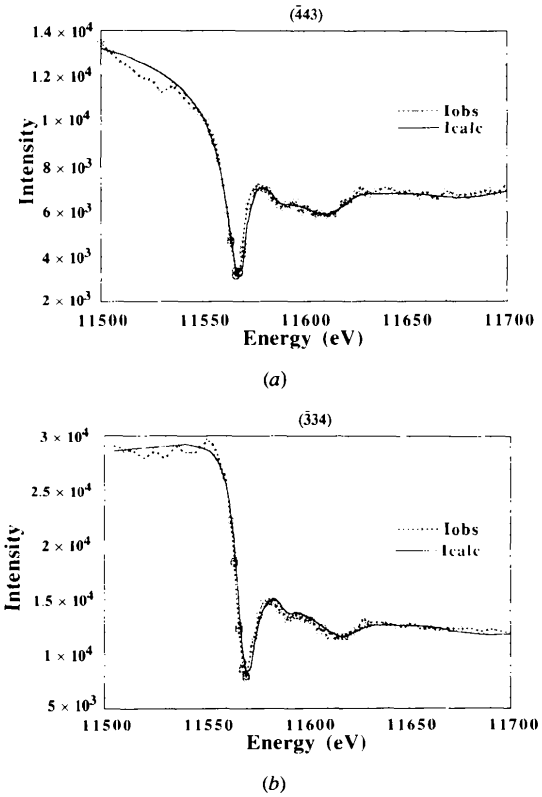

Figure 5
Raw intensity spectra of (hkl) reflections of the Ba–Pt–O compound as a function of the energy and the intensity fits applying the Lorentz–polarization, absorption and detector efficiency corrections. (*a*) Bragg reflection (4̄43) with dominant contribution of Pt cations. (*b*) Bragg reflection (3̄34) with dominant contribution of Ba atoms.

3.3. *Refinement of anomalous terms f′, f″ of different crystallographic sites from the diffraction signal*

The anomalous terms $f'_{Aj}(E_k)$ for different crystallographic sites j were calculated from the simultaneous refinement of all the measured Bragg reflections using the least-squares refinement program *MXD*. This program was originally developed for the refinement of crystallographic structures using data collected at one wavelength and we have modified it for the multiwavelength refinement of anomalous terms $f'_{Aj}(E_k)$. The non-linear system of kM equations with jk unknowns $f'_{Aj}(E_k)$, where k corresponds to the number of measured energy points and M to the number of Bragg reflections, was solved for the entire energy range measured. All the atomic parameters (positions and thermal factors), complex correction factors, absorption factors, Δt, y, detector efficiency D and Lorentz–polarization factors LP were fixed during the $f'_{Aj}(E_k)$ refinement. The initial average values of anomalous terms f' and f'' for all crystallographic sites included in the refinement were obtained either from theoretical curves for the free atom

(Sasaki, 1984) or from the transmission experiment with a powdered sample (f''_{trans}) and Kramers–Kronig relation (f'_{trans}). After each refinement procedure, the anomalous factors $f''_{Aj}(E_k)$ were calculated from the Kramers–Kronig relationship by the method described in the preceding paragraph and reintroduced into the refinement.

3.3.1. *$BaZnFe_6O_{11}$*. Using the anomalous scattering technique we have refined directly the population of Fe atoms on the mixed tetrahedral sites in $BaZnFe_6O_{11}$. The refinement gave the populations 0.79 and 0.38, which are comparable to the values 0.73 and 0.29 obtained by monochromatic refinement of a single crystal from the same batch. The anomalous terms f'_{tetra} and f'_{octa}, corresponding to the contributions of Fe atoms in tetrahedral and octahedral crystallographic sites, were refined in the energy interval 6900–7700 e V. Comparing the nine different Bragg reflections measured using the multi-monochromatic mode, we can select those which exhibit strong anomalous effects from others which have only a weak contribution from Fe atoms to the diffracted intensity and show only the intensity variation caused by bulk absorption effects (Fig. 6).

For calculations of the anomalous term f'_{octa} of octahedral sites and f'_{tetra} of tetrahedral sites we have used a weighting procedure which decreases the influence of strong Bragg reflections on the refinement. The anomalous terms f''_{octa} and f''_{tetra} were calculated using the Kramers–Kronig relationship. The resulting anomalous factors of tetrahedral f'_{tetra}, f''_{tetra} and octahedral f'_{octa}, f''_{octa} crystallographic sites, compared with the average values f''_{trans}, f''_{trans} obtained from the transmission XAFS experiment and the Kramers–Kronig relation of $BaZnFe_6O_{11}$ are shown Fig. 7. We can see on the f''_{octa} curves the intense white line at 7134 eV corresponding to the Fe atoms of octahedral sites and the different DANES (diffraction anomalous near-edge structure) oscillations for the two crystallographic sites.

3.3.2. *$BaPt^{4+}_{0.5}(Pt^{2+}_{1-y}Ba^{2+}_{y})_{0.25}O_{2.25}$ with $y=0.08$*. As in the case of the Ba–Zn–Fe–O system, the structure of the Ba–Pt–O compound contains two different crystallographic sites, octahedral (O) and trigonal prismatic (P), occupied by Pt^{4+} and Pt^{2+} cations, respectively. The refinement of the anomalous terms f'_{octa} (Pt^{4+}) and f'_{prism} (Pt^{2+}) of the Ba–Pt–O single crystal were performed using the energy interval 11500–11700 eV over the Pt L_{III} absorption edge.

First, refinements were performed with independent variables $f'_{octa}(E_k)$ and $f'_{prism}(E_k)$. Because of the weak contribution of Pt^{2+} cations in the prismatic sites, caused mainly by the disorder in the structure, an insignificant $f'_{prism}(E_k)$ curve was observed. As observed in the monochromatic refinement (Vacínová, Hodeau & Chamberland, 1994), the structure of the Ba–Pt–O compound contains twinned domains and translation faults due mainly to the P site positions with respect to the O site. Furthermore, each prismatic P site gives three possibilities of occupation by Pt^{2+} cations on one of the three rectangular faces of the prism and, in addition, there exists the mixed occupancy between Pt^{2+} and Ba^{2+} cations. This disorder also affects the anisotropy of the square-planar complex $(Pt^{2+}O_4)^{6-}$ characteristic for Pt^{2+} cations which was observed by Templeton & Templeton (1985) on the tetrachloroplatinate compound containing the $(Pt^{2+}Cl_4)^{2-}$ complex. It is possible that some of the Pt^{2+} cations contribute to diffuse scattering. To verify the weakness of the Pt^{2+} contribution

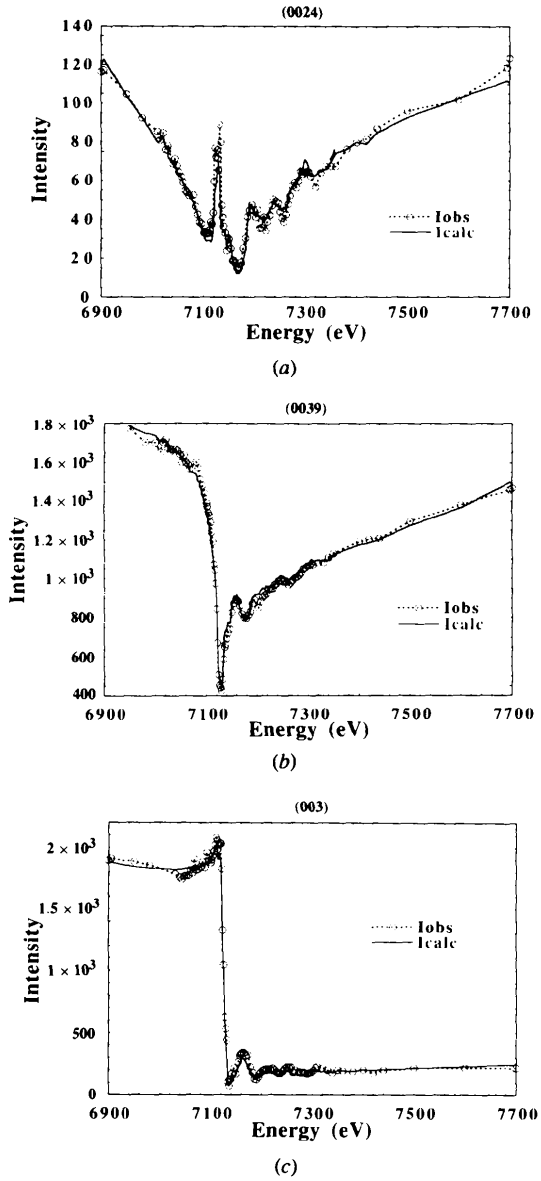

Figure 6
Intensity scan of Bragg reflection (*hkl*) *versus* energy of the Ba–Zn–Fe–O compound and the intensity fit using the known crystallographic parameters, f'_{Fe} and f''_{Fe} refined from DAFS data and f', f'' anomalous terms of Ba, Zn and O of free atoms (Sasaki, 1984). (*a*) Bragg reflection (0024) having the weak intensity and exhibiting very strong anomalous effects. The peak at the edge and the surprising shape of the intensity curve is due to the permutation of F_T and F_A contributions. (*b*) Bragg reflection (0039) with the strong contribution of Fe atoms. (*c*) Bragg reflection (003) having a strong intensity; the variation of intensity is mainly caused by bulk absorption effects.

in the diffracted intensities, we have performed calculations of: (i) $f'_{octa}(E_k)$ using only those Bragg reflections which have a dominant Pt^{4+} contribution, (ii) $f'_{octa}(E_k)$ using all 22 measured Bragg reflections, (iii) $f'_{average}(E_k)$ common for both Pt^{4+} and Pt^{2+} cations with all Bragg reflections.

With respect to the accuracy of statistical noise, the two curves $f'_{octa}(E_k)$ and the curve $f'_{average}(E_k)$ show the same features (the intensity and position of white lines, the DANES oscillations). The anomalous term $f'_{octa}(E_k)$ refined from all the reflections and $f''_{octa}(E_k)$ calculated by the Kramers–Kronig relation are compared with f'_{trans}, f''_{trans} obtained from transmission XAFS experiment as shown in Fig. 8.

The anomalous terms f'' for Pt^{4+} an Pt^{2+} powdered standards obtained from the transmission absorption spectra measured at ESRF at CRG French beamline IF-D32 are shown in Fig. 9. The differences between the anomalous terms f'' for Pt^{4+} and Pt^{2+} cations which we have observed on these Pt^{4+} and Pt^{2+} standards are mainly in the intensity of the white line and the features of the first DANES oscillations.

In the absorption spectra of the standards, we have also observed a small energy shift of ~ 0.5 eV between the Pt^{4+} and Pt^{2+} curves, which is the same order of magnitude as the energy resolution of the experiment. As seen in Fig. 8, the white line and the first DANES oscillations of the f''_{octa}

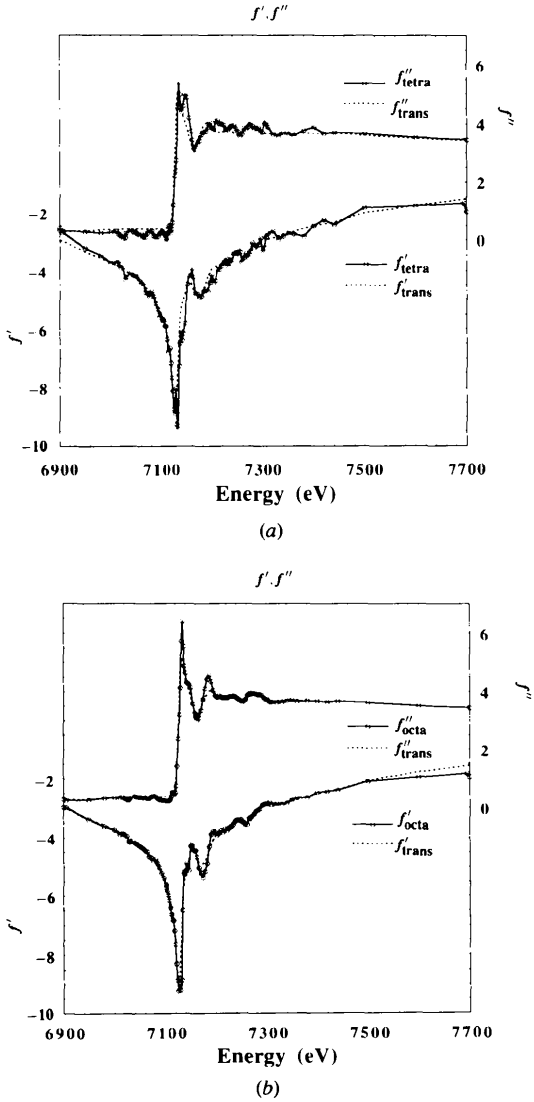

Figure 7
(*a*) Anomalous factors of tetrahedral crystallographic site f'_{tetra} refined from the DAFS signal and f''_{tetra} calculated by the Kramers–Kronig relation compared with the average terms f''_{trans}, f'_{trans} obtained from the transmission XAFS experiment with the $BaZnFe_6O_{11}$ compound and Kramers–Kronig relation. (*b*) Anomalous factors of octahedral crystallographic site f'_{octa} refined from the DAFS signal and f''_{octa} calculated by the Kramers–Kronig relation compared with the average terms f'_{trans} and f''_{trans}.

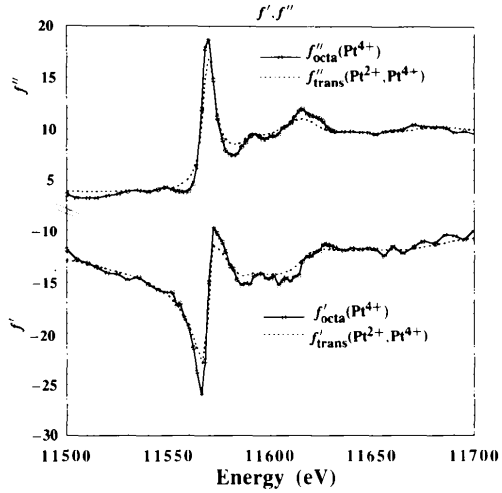

Figure 8
Anomalous term $f'_{octa}(E_k)$ of Pt^{4+} cations in octahedral sites refined from the anomalous diffraction signal and anomalous term $f''_{octa}(E_k)$ of Pt^{4+} calculated from $f'_{octa}(E_k)$ by the Kramers–Kronig relation compared with average anomalous terms f''_{trans} and f'_{trans} obtained from the transmission XAFS experiment with powdered sample and Kramers–Kronig relation.

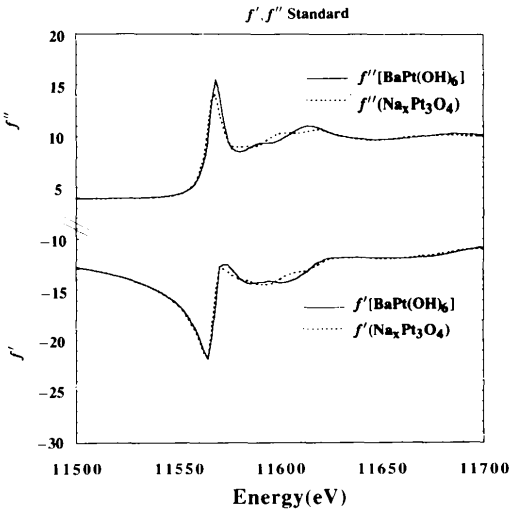

Figure 9
Anomalous terms f'' of Pt^{4+} [$BaPt(OH)_6$ (Bandel, Platte & Trömel, 1981)] and Pt^{2+} [$Na_xPt_3O_4$ (Schwartz *et al.*, 1982)] powdered standards obtained from absorption transmission spectra.

term are more pronounced than in the f''_{trans} curve probably because of the Pt^{2+} contribution in the transmission spectra.

4. Conclusions

We have applied the anomalous diffraction, DANES and DAFS techniques to the investigation of the local structure of anomalously diffracting atoms located in different crystallographic sites of 'real' oxides.

In the case of the Ba–Zn–Fe–O single crystal, the refinement of the anomalous f' curves corresponding to the contributions of the Fe atoms, situated in octahedral and tetrahedral crystallographic sites, was performed in the energy interval 6900–7700 eV (Fe K edge). The different anomalous terms f' and the terms f'' calculated by the Kramers–Kronig relation separate the characteristic features of the tetrahedral environment from those of the octahedral environment. The f' and f'' curves of both sites calculated from the DAFS signal are in good agreement with average spectra measured in the transmission absorption experiment with the powdered sample.

By using the same refinement procedure we have extracted the anomalous term f' of Pt^{4+} cations situated in the octahedral sites in the Ba–Pt–O compound at the energy interval 11500–11700 eV over the Pt, L_{III} absorption edge. Because of the local structural disorder of Pt^{2+} cations in this compound we could not obtain the anomalous term f' corresponding to the Pt^{2+} placed in trigonal prismatic sites. With respect to the anomalous term f'' calculated from the DAFS signal and the Kramers–Kronig relation, the term f'' obtained from the transmission absorption experiment shows a slight decrease of the white-line intensity and first near-edge oscillations corresponding to a mixed contribution of both Pt^{4+} and Pt^{2+} in the absorption spectra.

We have demonstrated the possibilities of the anomalous diffraction, DANES and DAFS methods on two examples of single crystals having complex structures (domains, twins, large unit-cell parameters) containing several crystallographic sites. We have developed an accurate absorption correction procedure for small, highly absorbing single crystals. This procedure can readily be extended to other single crystals by the determination of the empirical functions for each special case. Using the simultaneous multiwavelength refinement procedure of several Bragg reflections, we have calculated the anomalous terms f' of the anomalous atoms placed in different crystallographic sites directly from the DAFS signal. For the simplicity of the calculations the anomalous terms f'' were not refined as independent variables but calculated from the refined f' terms by the Kramers–Kronig relationship and then reintroduced into the refinements. This procedure of simultaneous refinement of several Bragg reflections shows the possibility of using DAFS methods on complex compounds in which none of Bragg reflections contains only contributions from the anomalous scatterers in a single specific crystallographic site. Hence, this procedure enables the use of anomalous scattering techniques for the structural determination and chemical analysis of complex mixed-valence oxides.

We would like to thank Dr J. L. Hazemann and Dr M. de Santis for their assistance during the transmission absorption experiments at ESRF, and Professors B. L. Chamberland, J. Muller and Dr A. Collomb for providing the crystals.

References

Bandel, G., Platte, C. & Trömel, M. (1981). *Z. Anorg. Allg. Chem.* **477**, 178–182.
Bearden, J. A. & Burr, A. F. (1967). *Rev. Mod. Phys.* **39**, 125–142.
Cauchois, Y. & Bonnelle, C. (1956). *C. R. Acad. Sci.* **242**, 1596–1599.
Collomb, A., Muller, J., Guitel, J. C. & Desvignes, J. M. (1989). *J. Magn. Magn. Mater.* **78**, 77–84.
De Bergevin, F., Brunel, M., Galéra, R. M., Vettier, C., ElKaïm, E., Bessière, M. & Lefèbvre, S. (1992). *Phys. Rev. B*, **46**, 10772–10776.
Kissel, L. & Pratt, R. H. (1990). *Acta Cryst.* A**46**, 170–175.
Pease, D. M., Brewe, D. L., Tan, Z. & Budnik, J. I. (1989). *Phys. Lett. A*, **138**, 230–234.
Pickering, I. J., Sansone, M., Marsch, J. & George, G. N. (1993). *J. Am. Chem. Soc.* **115**, 6302–6311.
Sasaki, S. (1984). *Anomalous Scattering Factors for Synchrotron Radiation Users.* National Laboratory of High Energy Physics, Japan.
Schwartz, K. B., Prewitt, C. T., Shannon, R. D., Corliss, L. M., Hastings, J. M. & Chamberland, B. L. (1982). *Acta Cryst.* B**38**, 363–368.
Stragier, H. (1993). PhD thesis, Univ. of Washington, USA.
Stragier, H., Cross, J. O., Rehr, J. J. & Sorensen, L. B. (1992). *Phys Rev. Lett.* **21**, 3064–3067.
Templeton, D. H. & Templeton, L. K. (1985). *Acta Cryst.* A**41**, 365–369.
Templeton, D. H. & Templeton, L. K. (1988). *J. Appl. Cryst.* **21**, 558–561.
Tröger, L., Arvanitis, D., Baberschke, K., Michaelis, H., Grimm, U. & Zschech, E. (1992). *Phys. Rev. B*, **46**, 3283–3289.
Vacínová, J., Hodeau, J. L. & Chamberland, B. L. (1994). *J. Solid State Chem.* In the press.
Wolfers, P. (1990). *J. Appl. Cryst.* **23**, 554–557.